Density Functional Theory Characterization and Descriptive Analysis of Cisplatin and Related Compounds

Pablo D. Dans and E. Laura Coitiño*

Laboratorio de Química Teórica y Computacional (LQTC), Instituto de Química Biológica, Facultad de Ciencias, Universidad de la República (UdelaR), Iguá 4225, 11400 Montevideo, Uruguay

Received November 13, 2008

Quantum and nonquantum descriptors clearly related to physicochemical features and predictors of the trends to evolve along different stages of a known mechanism of action were determined for a set of square-planar compounds of general formula $[M^{II}A_1A_2L_1L_2]$ (M^{II} = Pt(II)/Pd(II); A_i/L_i = carrier/labile ligands), structurally related to the anticancer agent Cisplatin. Selected compounds have been sorted and classified by Ward's Cluster Analysis and Principal Components Analysis data-mining techniques using seventeen 1D and two 3D of such theoretical descriptors calculated at the DFT level (PCM-B3LYP/LANL2DZ/6-31G*). A rationale emerging from the study is that whereas most significant differences come from substitution of Cisplatin ligands, *cis/trans* isomerism, and exchange of M^{II} introduce minor alterations in the electronic/geometrical structure. This provides theoretical support to the assay of transplatinum compounds as potential anticancer drugs, a fact already pointed out by empirical evidence. Similarly, the little geometrical/electronic differences triggered by switching M^{II} from Pt to Pd enable us to devise a rational path to propose new compounds with expected good anticancer profiles, tuning alterations introduced by simultaneously changing both metal and ligands. Current results serve thus to enlarge the Cleare-Hoeschele guides for Pt(II) square-planar anticancer potential drugs to Pd(II) compounds, both using *cis/trans* scaffolds.

INTRODUCTION

Cisplatin, a widely known anticancer drug, is employed in chemotherapy against different kinds of solid tumors.[1] Despite the remarkable success reached by its use several limitations are well documented along more than 30 years of clinical experience. Side-effects (gastrointestinal and kidney toxicity, immune system suppression, peripheral neurotoxicity, etc.) are dose-limiting disadvantages forcing the use of medical strategies to deal with their unpleasant consequences.[2,3] Inherent/acquired resistance considerably narrow the spectrum of malignancies to treat as well as the individual response obtained, whereas the biochemical mechanisms underlying these phenomena are not completely unraveled yet.[1,4]

The search of analogues to overcome these disadvantages led to approval of Carboplatin, a more soluble second generation Pt(II) species with better toxicological profile and similar antineoplastic clinical activity.[5] Outstanding efforts were devoted in the next decades to synthesize and screen a third generation of square planar Pt(II)/octahedral Pt(IV) related compounds (the latter rapidly reducing *in vivo* to Pt(II) species[6]). Based on a subtle balance between enhancement of anticancer activity, toxicological profile, and circumvention of drug resistance just a few compounds—Oxaliplatin, Nedaplatin, Lobaplatin, Satraplatin, and Picoplatin—emerged as promising candidates in phase III of experimentation against different malignancies[7,8] or even in clinical use (Oxaliplatin was approved by the FDA in 2002−2004 to treat colorectal cancer).[8b] According to the current knowledge all these drugs share a common mechanism of action leading to antineoplastic activity through covalent union of activated Pt(II) species—generated in the cell by S_N2 aquation processes—with genomic DNA, their pharmacological target. Whereas inter/intrastrand cross-links established between Pt(II) moieties and N7 atoms at DNA purines are the species to which cytotoxicity has been attributed, formation of covalent adducts and interactions with proteins and other relevant biomolecules is connected with adverse effects and resistance.[1,4]

Selection of new prospective drugs from thousands of prepared compounds is a relatively complex and low-efficiency task, essentially supported by experimental procedures aimed to screen activity profiles through *in vitro* and *in vivo* studies.[9] Systematizing indices from different sources and cell lines in a coherent outline reflecting effectiveness against tumors has not been easy to accomplish. Applying bioinformatics tools Fojo et al.[9] compared and clustered 107 platinum species from the National Cancer Institute's drug repository based on their *in vitro* anticancer profiles, finding 12 groups with a strong correlation with structural features. Application of robotic high-throughput screening and combinatorial chemistry tools to the systematic search of more effective compounds have produced so far few successful compounds, essentially helping to discard *in vitro* poor candidates.[9b,c]

The understanding gained on the molecular mechanisms of action,[1,3,4] the characterization of major DNA-Pt adducts, and the absence of antitumor activity of the *trans* isomer of Cisplatin[10] made it possible in the 1970s to establish a set of structure−activity relationships (SAR) known as the Cleare-Hoeschele rules.[11] Neutral square-planar Pt(II) complexes of general formula *cis*-$[Pt^{II}A_2L_2]$—A/L respectively

* Corresponding author phone: (+5982)-5252186; fax: (+5982)-5250749; e-mail: laurac@luna.fcien.edu.uy.

10.1021/ci800421w CCC: $40.75
Published on Web 05/22/2009

standing for inert am(m)ines/labile anionic (*i.e.:* chloride) ligands coordinated to Pt—were the structural motifs "required to guarantee" antineoplastic activity. Although these rules guided for years the design and synthesis of thousands of novel Pt(II) square-planar candidates, a realm of compounds defying them were also proved to display anticancer activity.[3,7,8] Alternative structural motifs include among others: *trans*-dichloroPt(II) species with different carrier ligands,[12] *cis*-$(NH_3)_2L_2$Pt(II) compounds with chelating leaving groups (L_2 = oxalate, glycolate, etc.),[7,8] *cis*-dichloroPt(II) species with secondary, tertiary, and/or heterocyclic amines acting as mono/bidentate ligands,[8b,13] octahedral Pt(IV) compounds, well suited for oral administration,[6,14] polynuclear charged platinum compounds,[15] and non-platinum metal-based compounds, particularly those of Pd(II) with bidentate amines, for which better toxicity profiles have been argued.[16] This points out the need and relevance of getting a wider perspective, looking for more detailed and complete characterizations of the known active compounds with the aim to classify them by structural themes. Then, this will help to elaborate more robust and representative structure—activity/reactivity-activity relationships, valuable in identifying structural motifs that should be taken into account in the future rational design of alternative compounds intended for clinical use.

Considerable efforts have also been devoted to characterize and predict the molecular mechanisms underlying the known anticancer profile of Cisplatin and congeners by applying both quantum and QM/MM theoretical methods[17−19] and molecular dynamics simulations.[20,21] There is a large amount of modeling studies on aquation processes,[17,20] DNA platination on systems of increasing complexity taken under more or less realistic conditions,[18,20b−d,21b−g] and chemical reactions presumed to be involved in developing toxic side-effects and resistance.[19] Although fundamental pieces of knowledge emerged from that work, a fairly reduced series of relevant Pt(II)/Pd(II) compounds has been examined thus far. A less explored way[22]—helpful in supporting the rational search of new drug candidates—is that of using theoretical methods and computational tools to determine quantum/nonquantum monodimensional (1D) descriptors clearly related to physicochemical features (*i.e.*: energy of frontier orbitals, solvent accessible surface areas, etc.) and 1D/3D predictors of the trends to evolve along different stages of the known mechanism of action (*i.e.*: charge reorganization/transfer accompanying molecular recognition/chemical transformations; nucleo/electrophilicity indices; etc.) to be used for establishing qualitative/quantitative structure−activity/structure-properties relationships.

Aimed to rationalize the available data to extend the rules guiding the search of novel potential anticancer drugs, we carried out a DFT comparative characterization of 35 Pt(II)/Pd(II) compounds (depicted in Figure 1) using a set of descriptive analysis to sort and classify them and to establish qualitative relationships between biological/pharmacological indices and calculated descriptors. The species are *cis/trans* square-planar complexes of general formula $[M^{II}A_1A_2L_1L_2]$ (M^{II} = Pt(II)/Pd(II); A_i = carrier ligand; L_i = labile ligand) obtained by introducing substitutions on the Cisplatin/Transplatin scaffolds (**1/1t** in Figure 1). A wide spectrum of anticancer activity profiles and relevant physicochemical properties (solubility, hydrophobicity, trend to react with biological nucleophiles through S_N2 processes, etc.) is covered: **1**, **15**, and **16** are worldwide established anticancer agents with well-known patterns of activity; **22** and **24** are used in clinical practice in Asian countries; **11** and **17** (a major metabolite of Satraplatin[6,29]) are in phase III of clinical experimentation, close to obtain FDA approval; **3**−**5**, **7**, **9**, **10**, **10t**, **12**−**14**, **17t, 18**, and **29** have displayed anticancer activity in preclinical assays.[7,8,16,23] **1t**, **2**, **2t**, **6**, **8, 19, 20** are known to be therapeutically inactive due to different reasons.[10,16] Biological/pharmacological anticancer activity indices are available from literature/open access databases only for a subset of the compounds,[13,16,24−31] lacking in any case from homogeneity (see Tables 1S and 2S in the Supporting Information for additional information on the anticancer activity profiles and indices). Thus, at this stage, just qualitative SAR/SPR relationships can be established on a firm basis on this set.

THEORETICAL AND DESCRIPTIVE METHODS

The structure of each member of the set has been fully optimized *in vacuo* at the DFT level without imposing constraints, using the B3LYP hybrid functional[32] with the 6-31G(d)[33] basis set for H, C, N, O, F, and Cl atoms and the LANL2DZ[34] pseudopotential and associated basis set for the transition metals (Pt/Pd). The nature of each optimized species has been carefully inspected checking the eigenvalues of the diagonalized Hessian. Solvent effects (water, ϵ=78.5) have been included at the same level of theory by single-point calculations using the PCM-IEF continuum model[35] with molecular shape cavities generated according to the United Atom Topological Model.[36] This combination of theoretical chemistry approaches has shown to have a very good performance in modeling structural characteristics and reactivity of this kind of compounds.[17d,j,k,o,18n,p,u,19c,f,37]

Seventeen structural and reactivity 1D descriptors have been obtained at the DFT/PCM level in aqueous solution including geometrical data (four metal−ligand bond lengths), molecular volume, solvent accessible surface area (SASA), natural atomic charges derived from Weinhold's NPA density population analysis[38] (6 by compound, corresponding to five atoms in the coordination sphere complemented by the most acid H in the amine moieties, which is presumed to play a central role in stabilizing metal-DNA interactions),[1,3,4] the energy of the Kohn−Sham's frontier orbitals (ϵ_{HOMO} and ϵ_{LUMO}), and the electronic chemical potential (μ), hardness (η), and electrophilicity (ω) calculated as reactivity descriptors in a conceptual DFT framework, within a finite differences method and frozen orbitals approach, according to the following expressions[39]

$$\mu = -\frac{1}{2}(\varepsilon_{HOMO} + \varepsilon_{LUMO}) \quad (1)$$

$$\eta = \frac{1}{2}(\varepsilon_{LUMO} - \varepsilon_{HOMO}) \quad (2)$$

$$\omega = \frac{\mu^2}{2\eta} \quad (3)$$

3D shape of the LUMO's electron density (taken as an approximation to the electronic Fukui's function)[39] and 3D molecular electrostatic potential (MEP) mapped on a isos-

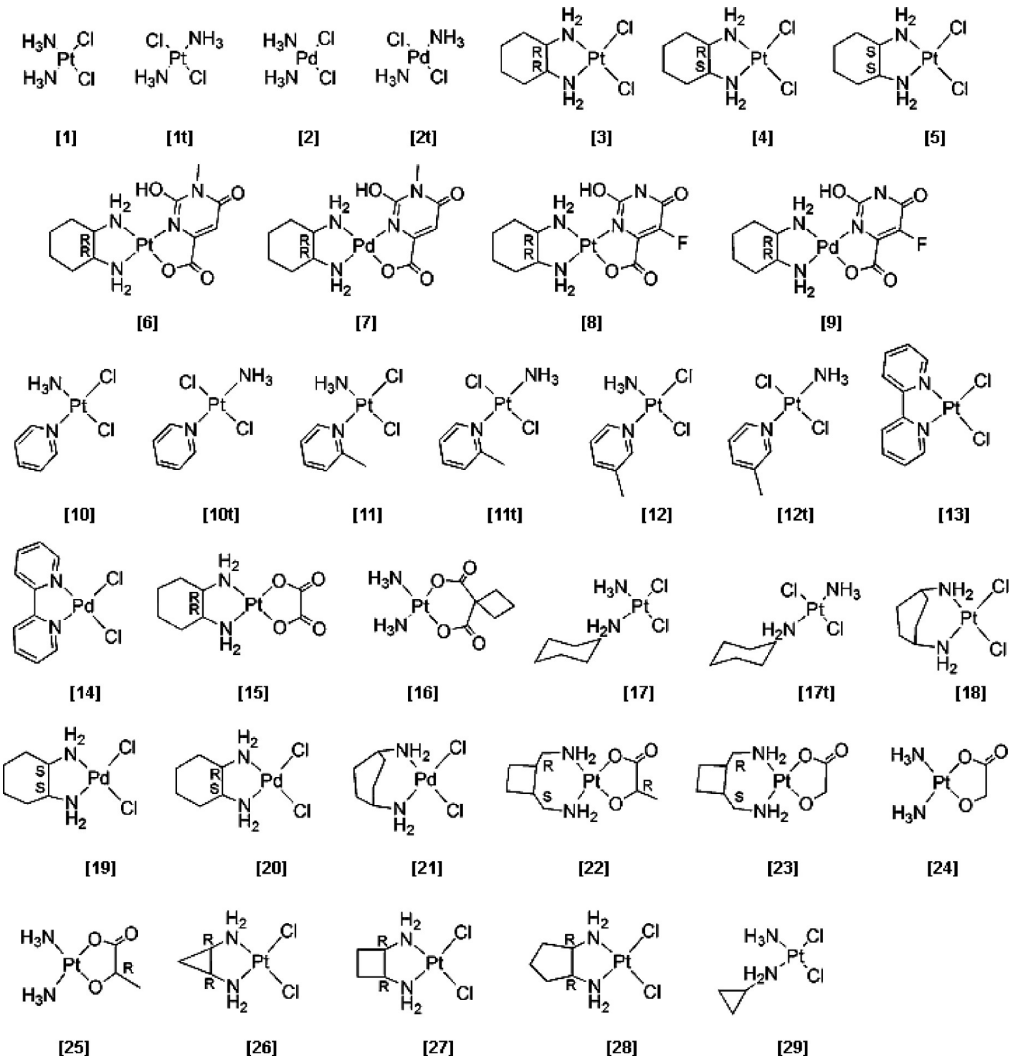

Figure 1. Sketch of the structures for the Pt/Pd *cis/trans* complexes under examination. See Supporting Table 1S for a detailed identification (chemical formulas, commercial/common names) and description of the known anticancer activity profiles for the 35 compounds.

urface of electron density (0.0004 au) have also been obtained, visualized, and analyzed as reactivity descriptors. All the descriptors were generated and/or graphically analyzed using Gaussian03 revision B05,[40] Gaussview 2.1[40b] and Molekel 4.3[41] programs.

A Hierarchical Cluster Analysis (***HCA***)[42] was performed on the 17 × 35 matrix of 1D standardized descriptors for the complete set of compounds, using the Chebychev algorithm to obtain a distance matrix. A dendrogram—displayed in Figure 2—was constructed for the 35 cases by using Ward's hierarchical agglomerative method[42] clustering the data set by proximity. A Principal Component Analysis (***PCA***)[43] was performed on the same 17×35 correlation matrix to condense information on shape and reactivity[44] into a new set of nonredundant variables (*Principal Components, PCs)*. *PCs* are linear combinations of the descriptors (related by means of weights *p,* the *PC loadings*) reflecting major physicochemical features of the species. Applying Kaiser's approach[43] only *PCs* with *eigenvalues >1* were retained in this work. The two *PCs* retained, used to generate *loading* and *score plots*, were selected as those that accumulate a maximum variability among compounds and have at least one original descriptor with *PC loading* $p \geq 0.8$. Similarities among the compounds can be detected and analyzed by means of their *scores* plotted on the *PC1* × *PC2* plane.

HCA and ***PCA*** were performed and visualized by using Statistica software.[45]

RESULTS AND DISCUSSION

Figure 2 shows the result of Ward's agglomerative clustering with cluster hierarchies visualized as a dendrogram. Whereas the complete matrix of theoretical descriptors is available as Supporting Information (Table 3S), a selection of representative values is collected in Table 1. Figures 3 and 4 respectively contain 3D isodensity representations of the LUMO and a selection of MEPs. *PCA* loading and scores plots for the compounds characterized are shown in Figures 5a-b and 6.

Hierarchical Cluster Analysis. All compounds were sorted on the base of their geometrical and electronic similarities/differences into well-defined clusters at different hierarchical levels, each of them represented by a tree branch in the dendrogram in Figure 2. Linkage distance at each branching makes it possible to assess the relative impact of introducing specific variations on the basic structural and reactivity motifs present in Cisplatin/Transplatin scaffolds. It is worth to recall here that covering a wide spectrum of anticancer responses, Fojo et al. found that platinum-based compounds belonging to a same group of distinctive activity patterns (clustered by similarity in activity profile against cell lines in NCI_{60}) undoubtedly share chemical structure features.[9]

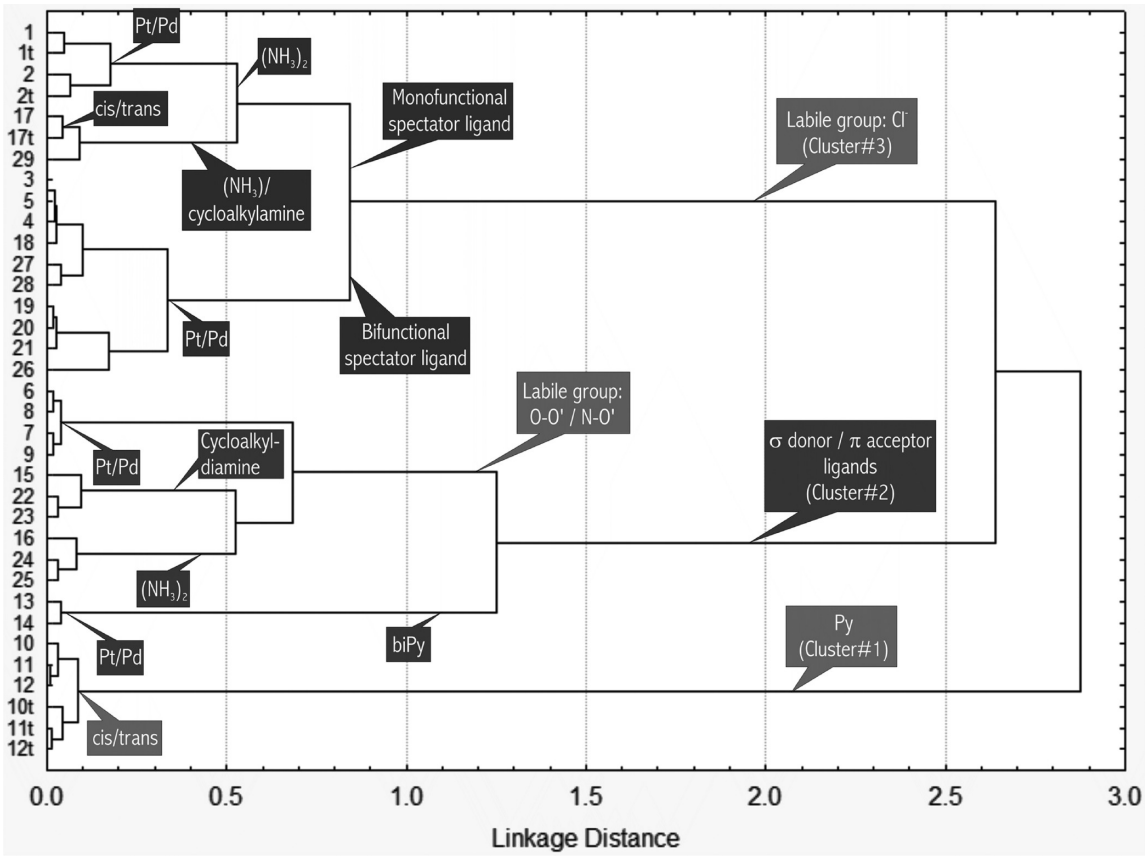

Figure 2. Dendrogram for the set of 35 compounds generated with Ward's hierarchical clustering, using 17 theoretical local and global descriptors. The numbers in the top of the figure identify the species according to the scheme in Figure 1.

Table 1. Selection of Theoretical Descriptors for a Set of Representative Compounds Grouped According to *HCA* Clusters[a]

cluster	compd ID	M	electronic chemical hardness(η)	electro-philicity (ω)	ϵ_{HOMO}(au)	electronic chemical pot. (μ)	ϵ_{LUMO}(au)	surface (Å^2)
#3 labile group	**1**	0.594	0.0891	0.253	−0.23929	0.150	−0.06118	172
Cl^- in the absence	**1t**	0.604	0.0842	0.249	−0.22896	0.145	−0.06055	173
of σ-donor/π-	**2**	0.667	0.0780	0.379	−0.25003	0.172	−0.09404	173
acceptor ligands	**2t**	0.671	0.0766	0.355	−0.24142	0.165	−0.08826	172
	17	0.587	0.0894	0.243	−0.23685	0.147	−0.05798	304
	17t	0.602	0.0843	0.238	−0.22589	0.142	−0.05732	273
#2 presence of	**6**	0.780	0.0853	0.328	−0.25247	0.167	−0.08196	369
σ-donor/ π-	**8**	0.782	0.0850	0.331	−0.25268	0.168	−0.08265	351
acceptor ligands	**7**	0.809	0.0875	0.337	−0.25915	0.172	−0.08422	368
	9	0.811	0.0861	0.340	−0.25712	0.171	−0.08502	351
	15	0.765	0.1013	0.177	−0.23537	0.134	−0.03278	351
	22	0.726	0.0944	0.113	−0.19760	0.103	−0.00875	275
	23	0.731	0.0940	0.115	−0.19788	0.104	−0.00997	246
	16	0.785	0.1037	0.169	−0.23600	0.132	−0.02857	254
	24	0.740	0.0939	0.126	−0.20245	0.109	−0.01467	172
	25	0.740	0.0943	0.122	−0.20158	0.107	−0.01291	197
	13	0.660	0.0725	0.393	−0.24136	0.169	−0.09634	327
	14	0.691	0.0763	0.392	−0.24920	0.173	−0.09666	291
#1 pyridine or	**10**	0.613	0.0893	0.252	−0.23915	0.150	−0.06061	260
derivatives as	**12**	0.612	0.0893	0.249	−0.23846	0.149	−0.05980	280
carrier ligands	**11**	0.610	0.0890	0.249	−0.23782	0.149	−0.05977	289
	10t	0.626	0.0835	0.265	−0.23230	0.149	−0.06533	238
	12t	0.625	0.0835	0.263	−0.23159	0.148	−0.06456	263
	11t	0.624	0.0837	0.251	−0.22858	0.145	−0.06111	256

[a] For the complete matrix for all compounds, see the Supporting Information (Table 3S).

The most remarkable fact emerging from Figure 2 is the neat differentiation from the rest of the set of those compounds with pyridine planar amines as monodentate carrier ligands, namely *cis* species **10**−**12** and *trans* species **10t-12t**, identified as ***Cluster#1*** and labeled ***Py*** in the figure. The uniqueness in structural—both geometrical and electronic— and reactivity characteristics evidenced by this analysis matches the differential behavior in anticancer profile

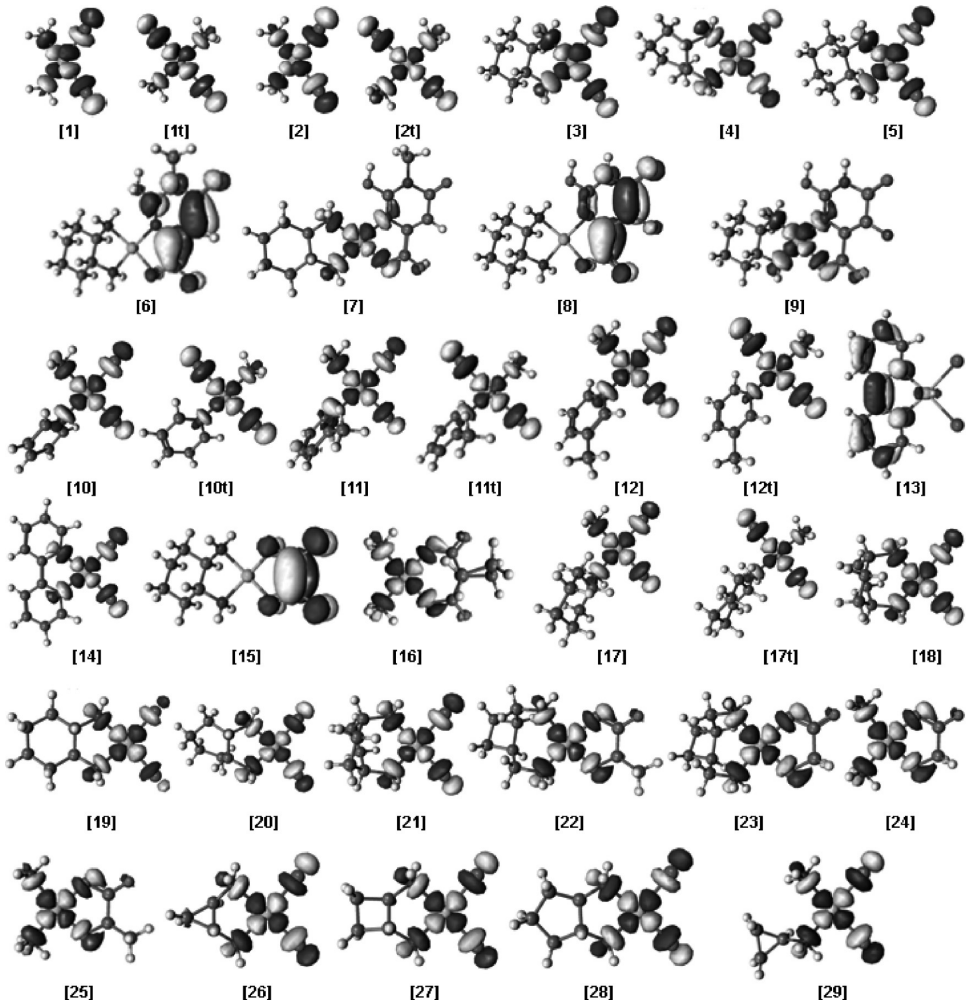

Figure 3. 3D representation of the Kohn−Sham LUMO orbital obtained at the PCM-IEF/B3LYP level. Isodensity contours are depicted for a value of 0.0004 au KS LUMO+1 for compounds **6**, **8**, and **15** (shown in Supporting Figure 1S) resemble in shape the σ^* LUMOs here depicted for the rest of the set, destabilized by amounts of ∼0.99 eV in the case of both orotic acid derivatives and 0.16 eV in the case of Oxaliplatin (**15**).

found for these compounds, currently under testing with the specific aim of overcoming cross-resistance with well established anticancer drugs.[9,13]

At a first glance, a second level of branching would distinguish among species bearing labile ligands other than chloro (***Cluster#2***) and those with Cl^- leaving groups (***Cluster#3***), where compounds **13** and **14** (*biPy* in Figure 2) appear to be an exception to this rule. A closer look into the structural features of the species in ***Cluster#2***—the richest in established anticancer agents—enables to recognize the presence of N−N′, N−O, and/or O−O′ chelating ligands, sharing the ability of acting both as σ-donors/π-acceptors, as the actual sorting motif. This kind of ligands can delocalize electron density away from the metal center through π back-donation effects,[46,46b] as evidenced by a more positive charge on M compared to Cisplatin (see data in Table 1).

As can be seen from Figure 3, all the known cytotoxic species in ***Cluster#2*** (**7**, **9**, **14**, **16**, **22**, and **24**) but Oxaliplatin (**15**) exhibit chemically active σ-antibonding LUMOs involving a metal *d* state and ligand orbitals. This is an electronic signature shared by all the anticancer agents across ***Clusters#1−3*** for which biotransformation is initiated by S_N2 reactions with water and biologically active species. Oxaliplatin's LUMO, a π-antibonding KS orbital spread over the oxalate leaving group, definitely constitutes a distinctive electronic characteristic of this antineoplastic agent. This feature, in conjunction with its quite less electrophilic character relative to Cisplatin (see ω values in Table 1), could be in the roots of the particular tumor selectivity and the lack of cross-resistance allegedly[47a] displayed by Oxaliplatin. This gives indeed sustain to the possibility of alternative mechanisms of action in the body, triggered by noncovalent interactions with biomolecules (a fact already pointed out by the empirical research conducted in the case of *biPy* compounds).[16b−d] The two known inactive Pt(II) species within this branch (**6** and **8**) also exhibit π-antibonding LUMOs located over their corresponding orotato ligands, a characteristic promptly removed by substitution of Pt(II) by Pd(II), to give the cytotoxic charged species **7** and **9**. A similar pattern can also be observed in passing from Pt(II) **13** to Pd(II) **14** more cytotoxic species. The next higher KS orbital resembling the LUMO usual shape observed in platinum anticancer drugs is the LUMO+1 for the case of **6**, **8**, and **15,** and the LUMO+3 for **13**—see Supporting Information Figure 1S. These KS orbitals are respectively 0.99, 0.99, 0.16, and 1.21 eV higher in energy than the corresponding LUMOs. These energy gaps show the distinctive LUMO not to be an artifact of the calculation for **6**, **8**, and **13**. For Oxaliplatin, the gap between the two electronic states is close to the bounds of expected error of the model.

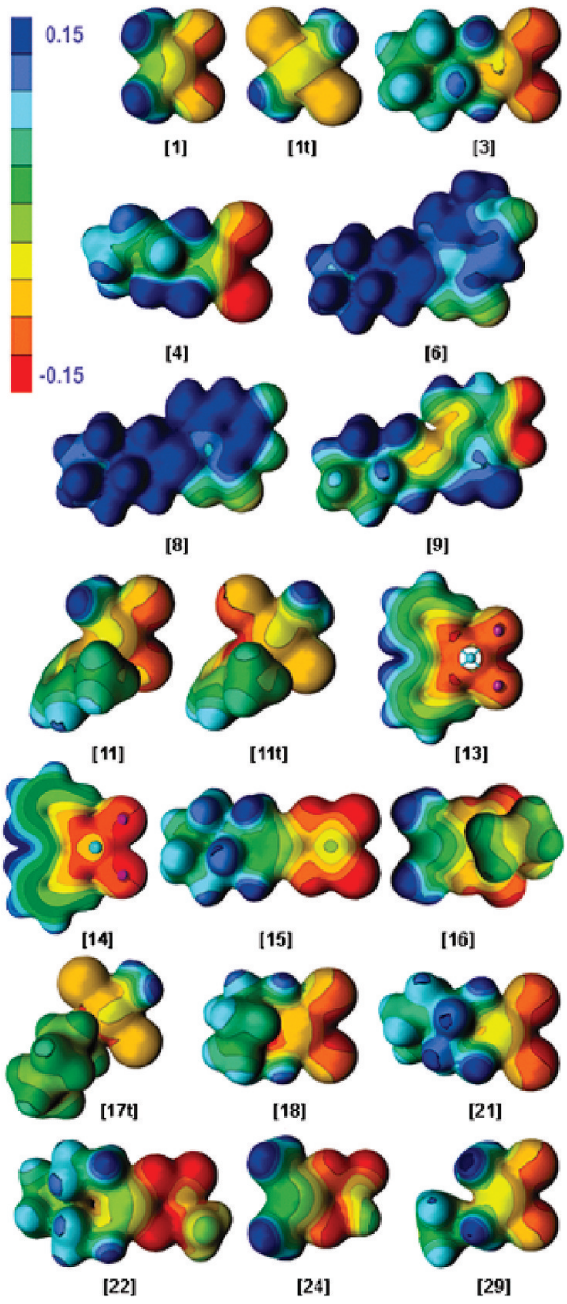

Figure 4. Selection of representative 3D Molecular Electrostatic Potential (MEPs) mapped on an electron density surface of 0.0004 au. Scale of colors from red to blue represents MEP values ranging from −0.15 to +0.15.

Examination of the 3D mapped MEPs depicted in Figure 4 enables to complement these considerations. Whereas *in vitro* cytotoxic species exhibit a pronounced gradient from the region around the metal center M to both the surface of carrier and labile ligands (responding to the picture of highly polar molecules, containing large areas of both positive and negative potential), Pt(II) inactive (**6** and **8**) and low-cytotoxic (**13**) species display a fairly more homogeneous distribution of charge around M. This distinctive feature in the case of Pt(II) species switches again to the more common pattern (pronounced electrostatic potential gradient) when tuning the electronic density by substitution of the metal center by Pd(II) (see pairs **6**→**7**; **8**→**9**; **13**→**14**).

These pieces of evidence clearly support the idea that an adequate interplay between the effects of changing the nature of the ligands and charge on M might be a promising strategy for tuning the electronic features of square planar compounds in order to obtain cytotoxic species with a particular anticancer profile. In the case of Pd(II) square planar compounds, modulation of the well-known activating effect of Pt(II)/Pd(II) substitution can be achieved comprising in the structure stabilizing σ-donor/π-acceptor chelating ligands.

The most important level of distinction within ***Cluster#3*** (species with Cl^- as labile group in absence of σ-donor/π-acceptor ligands) corresponds to the bidentate/monodentate nature of the carrier ligands, respectively reflecting the presence/absence of cyclometalation effects[46c,d] as the main discriminating motif. Inspection of further sub-branching shows that albeit a Pt(II)/Pd(II) exchange has a profound impact on kinetics of the S_N2 processes involving Cisplatin, geometrical and electronic alterations caused by metal substitution are relatively minor in comparison to the changes introduced by replacing the leaving group/carrier ligand. Something similar happens with the effects of introducing *cis/trans* variations.

Theoretical support is thus provided here to the need of enlarging the rational rules initially proposed by Cleare and Hoeschele[11b,c] to also include *trans* species in which the choice of L1-L2 and carrier ligands is conveniently done to achieve a balance among the structural modifications—steric and electronic—that modulate the desired properties determining the activity profile. In the search of new pharmacological leads with specific anticancer sensitivity, toxicity and resistance features, virtual screening supported by a ***HCA*** based on 1D theoretical descriptors of clear physicochemical meaning (coupled with the analysis of 3D descriptors) is shown to be a powerful aid in sorting and recognizing common patterns over wide sets of possible candidates and expanding or extracting new rationales to guide further synthesis research.

Principal Component Analysis. Two principal components, labeled *PC1* and *PC2* in Figures 5 and 6, emerged from ***PCA*** with *eigenvalues* of respectively 4.2 and 2.2, to which 64.34% of the variability among compounds can be attributed. Examination of Figure 5a immediately brings to the attention that the local descriptors corresponding to the carrier ligands have small *loadings* in both *PC* ($p \leq |0.5|$). *PC1*, accounting for the 42.34% of the total variability, explains differences among compounds along the horizontal axis in Figure 5b. It essentially responds to global descriptors of molecular stability and reactivity and local descriptors associated to the labile ligands. $\epsilon_{LUMO,}$ hardness (η), and ϵ_{HOMO} exhibit positive *PC* loadings; electronic chemical potential (μ, the opposite of the electronegativity χ), electrophilicity (ω), L1/L2 atomic charges and M-L1/M-L2 bond lengths, possess negative loadings. Thus—provided that axial steric hindrance is not present—in moving from the left to the right it would be expected to find compounds with stronger M-L interactions, progressively becoming less reactive toward S_N2 biotransformations, less prone to establish covalent interactions, and more electronegative.

Reminding that the *in vitro* anticancer activity has been linked by Monti et al.[25] to the optimization of the difference in χ between atoms separated by 3−4 bonds, and also by us (see previous discussion) to a pronounced gradient of MEP between the accessible regions on the carrier and labile ligands, *PC1* can be roughly interpreted as reflecting a

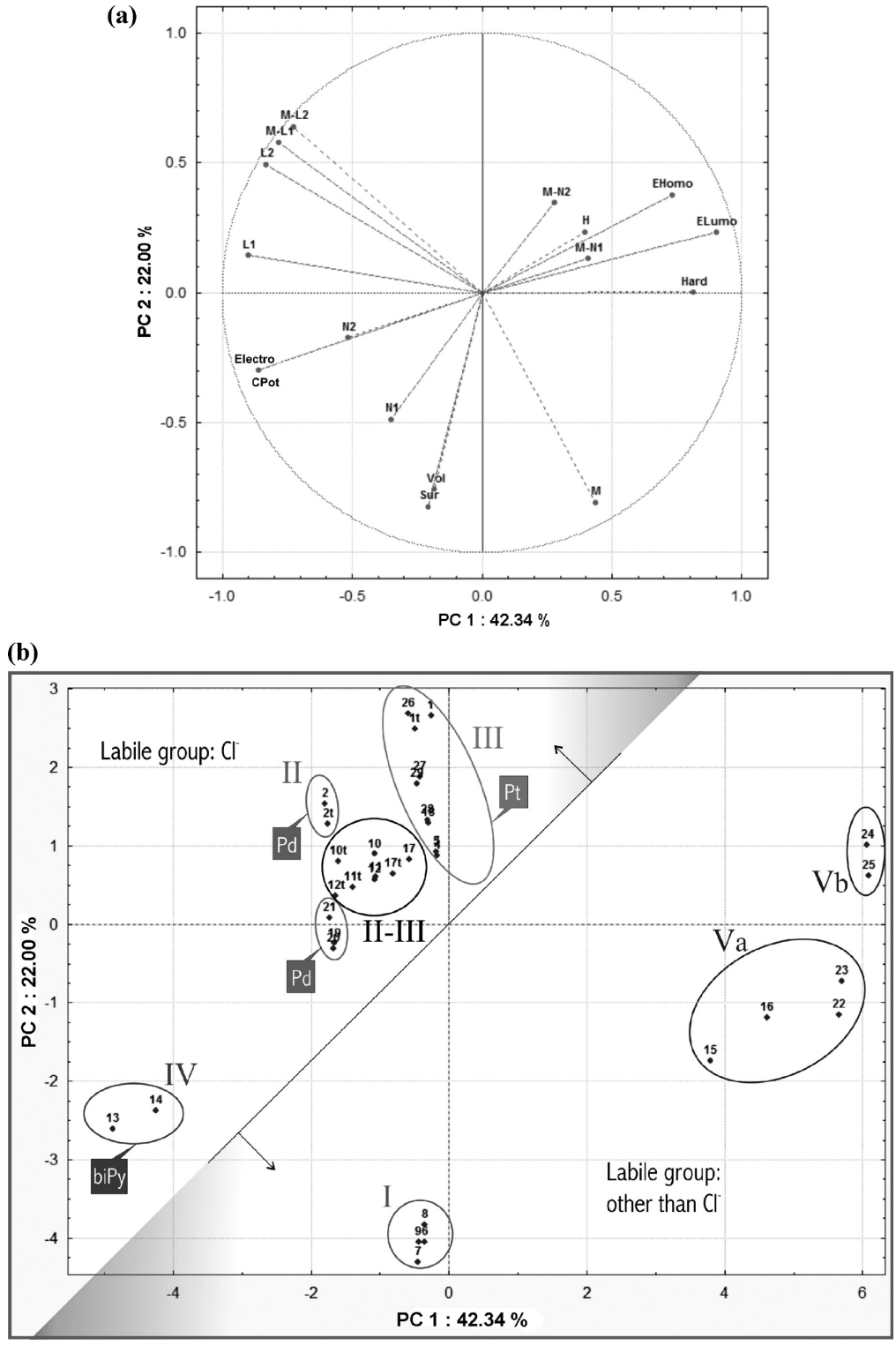

Figure 5. a. ***PCA*** loadings plot for *PC1* and *PC2*. List of acronyms used for the 17 descriptors: ***Sur*** = solvent accessible surface area; ***Vol*** = molecular volume; ***M-X*** = bond length for metal center (M) binding to each of the four atoms in the first coordination sphere (X = L1, L2, N1, N2); ***M, N1, N2, L1, L2, H_{ac}*** = NPA atomic charges; ***EHomo/ELumo*** = HOMO/LUMO orbital energies; ***Electro*** = electrophilicity; ***Hard*** = chemical hardness; ***CPot*** = electronic chemical potential as defined in the text. b. ***PCA*** score plot derived from a 35 compounds × 17 descriptors matrix. A classification of the compounds in five groups (I, II, III, IV, and V) is shown. Identification of each compound follows numeration scheme provided in Figure 1.

delicate balance between contributions to systemic toxicity and anticancer cytotoxicity (which also related to the features of the activated form of the drug, available to attack DNA within the cellular context). That means that whereas compounds placed to the right would be, in principle, quite less toxic and variable in efficacy compared to Cisplatin (constituting a space of improved tolerability, as anticancer agents in ***Group V*** actually do) species located nearby the central region in the plot—***Groups I*** and ***III*** in Figure 5b—would be expected to display toxicity and activity close to those of Cisplatin, constituting a space of structural chemotypes for which cancer sensitivity and selectivity

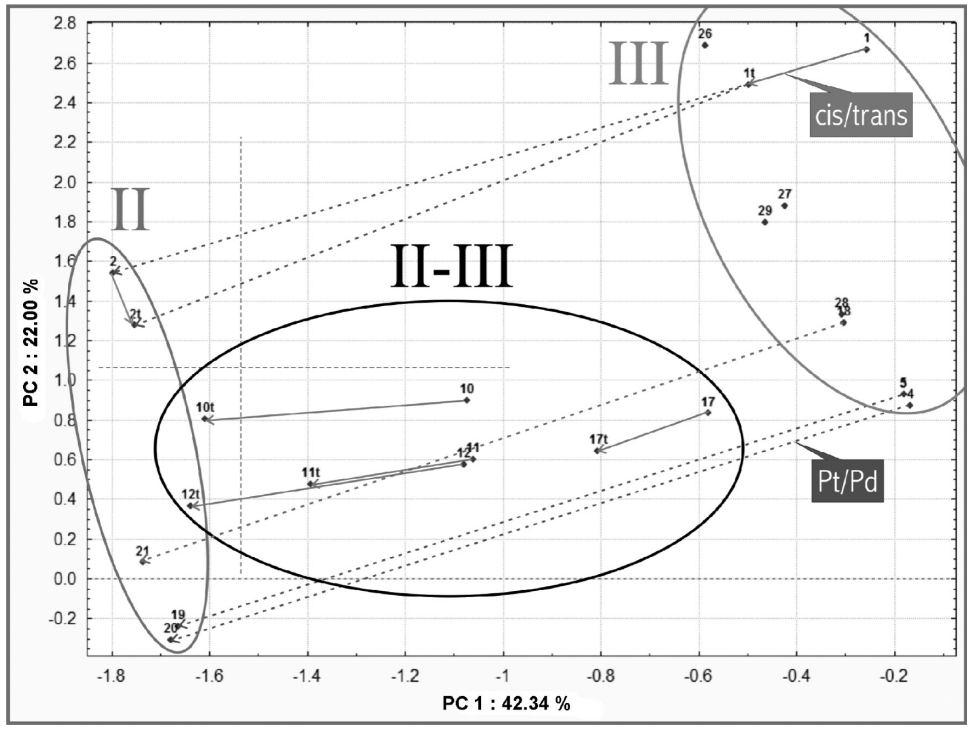

Figure 6. Enlargement of the ***PCA*** Scores Plot section corresponding to the projection of compounds in Groups II, II−III, and III. Solid arrows connect *cis/trans* pairs of isomers; dashed arrows connect Pt(II)/Pd(II) counterparts.

should be tuned by optimization of other orthogonal molecular features, contained in one or more of the remaining *PCs*. The region placed at more negative values of *PC1*—populated here by ***Groups II*** and ***IV***—would represent a space of quite toxic compounds whose kinetic stability could be not enough to ensure the compound arrives to the cell to lesion DNA.

This ordering reproduces well the observed anticancer responses of each clinical agent and tested compound for all the species in the set but **10**−**12**, **16**, and **17** (and their respective *trans* isomers, where applies) which are essentially gathered in ***Group "II*−*III"***, misplaced in Figure 5b. These compounds bear bulky moieties lying above/below the molecular plane, which block the S_N2 entering channel in a way that preferentially reduces reactivity toward soft nucleophiles. Reflecting this feature (not contemplated in the theoretical descriptors in *PC1* and *PC2*) on the location of such species would require to shift them rightward in Figure 5b, toward the improved tolerability region, adopting *PC1* effective values higher than that of Cisplatin.[13,13b,14]

The properties explaining differences along the vertical axis given by *PC2* (accounting for 22.00% of the variability among compounds) are the charge on M and the molecular surface and volume of the species (respectively *Sur* and *Vol*), all with negative loadings in Figure 5a. In going from top to bottom in Figure 5b, compounds become larger—and thus more hydrophobic—and M increases from +0.59 up to +0.81 au. This *PC* could be interpreted as explaining part of the variability associated to cellular drug uptake and efflux, two features known to exert a deep influence on cellular sensitivity to the drug and resistance patterns.[1,14,29b,48−50]

It has been shown that Pt cellular accumulation correlates with hydrophobicity (expressed in terms of $\log P_{o/w}$, as a good predictor of the entrance of platinated drugs to the cell since correlates with platinum uptake[27] and this, in turn, to the molecular area[22b,d]) in a differential way in sensitive/resistant cells.[48c,d] Thus, going down along *PC*2 would follow the trend of increasing hydrophobicity and enhancing passive diffusion into the cell as a mean to bypass resistance due to reduced facilitated uptake. On the other hand, specific interactions with metal binding domains of several cellular transporters having a role in mediating platinum inward flux (copper homeostasis proteins[49] and organic cation transporters,[50] among others) would be modulated by the molecular size and shape of the drug as well as by the charge on the metal and the electrostatic features on the accessible surface (shown in Figure 4). Encompassed with a deeper knowledge on the structural determinants of substrate specificity and the expression of transporters in normal/malignant tissues, the organization of compounds along *PC2* might be conveniently exploited, in conjunction with MEP and LUMO 3D descriptors, to perform *in silico* preselection of new promising candidates sought to bypass cross-resistance with Cisplatin or even addressed to treat unresponsive malignancies expressing cell-type specific transporters.

Oxaliplatin can be taken here as an archetypal case to validate the general procedure of using a ***PCA*** based on these physicochemical descriptors with predictive purposes. The species is located at the region of improved tolerability along *PC1,* and has the lowest projection on *PC2* among those of the platinum clinical agents in the score plot. Besides its LUMO's uncommon features, additional singularities in features defining the nature of the interactions the drug can establish with proteins (transporters in particular) are exposed with the analysis. Experimental evidence supports now multiple cellular transport systems for Oxaliplatin which appear to be distinct from those of Cisplatin, Carboplatin, and Nedaplatin, a finding that has been invoked as one of the reasons to explain its singular efficacy against colorectal cancer.[49b,50]

Separation among groups of species according to the nature of the labile ligands L is clearly evidenced in the score plot in Figure 5b, which is divided by a wide diagonal region placed in between of two populated zones (one includes ***Groups II−IV***; the other ***Groups I*** and ***V***). This illustrates how the use of bulky chelating L can be exploited as an efficient strategy to modulate systemic toxicity and/or cell uptake of *in vitro* active compounds typical of ***Groups III*** and ***IV***. Since experimental evidence sustains that compounds in ***Groups I*** and ***V*** are activated through biotransformation processes before reaching its molecular target, their Cl^- congeners (such as **1** and **3**) would be more representative to anticipate their *in vivo* cytotoxicity, being thus the former considered as precursors or pro-drugs.[47b]

To conclude, a global examination of the constitution and location of the six groups identified across the ***PCA*** score plot (Figure 5b) and the three main clusters emerging from ***HCA*** (Figure 2) can be performed to integrate and compare both analysis. Compounds in ***Cluster#1*** and ***Cluster#3*** essentially concentrate at the left upper quadrant, in a disposition that completely masks the singular characteristics of Pt(II) pyridine derivatives (particularly their lower reactivity toward thiol-containing species) readily evidenced by ***HCA*** and linked to their unique anticancer profile (partial/full noncross-resistance to Cisplatin, Carboplatin, and Oxaliplatin in pretreated lung, colon and ovarian malignancies).[13] Once the reduction in reactivity by axial sterical hindrance is reflected by shifting the location of ***Group "II−III"*** rightwards along *PC1*, the *Py* structural chemotype appears as one of the few populating the right upper quadrant in the scores plot. These compounds have hydrophobicity and M values intermediate between those of Cisplatin and those of the other clinical agents in ***Group V***, sharing these features with JM118's cyclohexylamine motif (species **17,** assigned to ***Cluster#3*** in the ***HCA***). Cellular pharmacology of JM118 is currently attracting attention because of the finding that very different cellular mechanisms of resistance respect to Cisplatin are engaged with it, being apparently able to hypersensitize cells to other nonplatinum anticancer drugs.[49c] Compounds previously gathered in ***Cluster#2*** are, in general terms, contained in three groups spread all over the bottom of the scores plot, covering the three regions of toxic side-effects/anticancer activity balance previously identified along *PC1* and also displaying significant differences between them along *PC2*.

Whereas the impact of Pt/Pd substitution has different magnitude depending on the family of compounds considered (being more important for species belonging to **Cluster#3**, a fact that is better appreciated in Figure 6) the general trend is, as expected, to shift toward regions of lower values both in *PC1* and *PC2*. This mainly reflects the more electrophilic character of the Pd counterpart and the increasing positive charge on the metal. The effect is quite less significant for species in ***Cluster#2***, noticing that in the case of compounds **13/14** (***Group IV***) a reversion in the general trend in both *PCs* is even detected. This reaffirms the idea that, although not advisible for the simplest Pt scaffolds included in ***Group III*** because of the excessive activation gained, Pd substitution can be a convenient strategy in tuning properties and response of metal-based square planar compounds used together with stabilizing chelating labile groups or π-acceptor moieties. Regarding the *cis/trans* effect, as can also be seen in Figure 6, a similar pattern in shifts over the *PC*1x*PC*2 plane is found, although the changes are quite less significant yet and the effect seems to be more pronounced in platinum species belonging to ***Cluster#3***.

CONCLUSIONS

A reduced set of theoretical global and local physicochemical descriptors, calculated at the DFT/PCM level, with a clear connection to the structure, stability and intrinsic reactivity of M^{II} coordinated square planar complexes (M = Pt(II)/Pd(II)) has been used here to describe and sort by ***HCA*** and ***PCA*** data-mining techniques a group of 35 compounds structurally related to Cisplatin, most of them displaying *in vitro* anticancer activity and some currently in clinical use as antitumor agents for different kind of human malignancies.

HCA has shown to be a very useful tool to retrieve meaning from a subset of the 1D calculated physicochemical descriptors and to sort the species in clusters related to particular anticancer profiles, well-defined in terms of potency, side-effects and resistance patterns, in a way that immediately points out the singular characteristics of compounds bearing monodentate pyridines as carrier ligand—Picoplatin in this group—which indeed constitute a promising chemical space for further exploration and lead optimization. Exploited in a complementary way with the use of surface mapped MEPs and KS LUMOs as 3D descriptors, ***HCA*** becomes a very useful, cheap and efficient strategy for performing *in silico* preselection of new antitumor candidates within large amounts of compounds representative of several chemotypes combining multiple variations. On the other side, ***PCA*** enables to perform a more detailed level of analysis, explaining differences within each cluster and putting in evidence the existence of different chemical spaces reflecting the result of a subtle balance between improved cytotoxicity/tolerability (reached by tuning the species reactivity and surface MEP gradient) altogether with the ability of the compound to enter the cell through active/passive diffusion processes and reach its final molecular target.

A measure of the impact of introducing different kinds of structural changes is also given here. Despite the known effect on kinetics of Pt/Pd and *cis*/*trans* variations, the combination of descriptors and data mining techniques used herein has shown them to be of minor impact on determining similarities/differences among these compounds. Introducing σ-donor/π-acceptor stabilizing chelating moieties emerges as one of the most influential variations to apply (especially at the labile positions) on the structural platinated square planar scaffold, followed by the effect of a cyclometalation/monodentate-binding interplay at the carrier ligands. This work provides thus a rational base to enlarge the preestablished SAR rules including *trans* motifs or M=Pd(II) as chemotypes for searching new leads, provided an adequate balance in kinetics is obtained by tuning the nature of the carrier and leaving groups and/or blocking the S_N2 entering channel by introducing bulky substituents in the ligands. Along with the known biological activity of each compound this study enables to device a rational path to propose new candidates with expected good anticancer profiles.

ACKNOWLEDGMENT

This work has been financed by CSIC-UdelaR through Research & Development (ELC, 2000-2002) and Young-Researchers (PD, 2003−2004) programs. Sustained support from PEDECIBA (PNUD-UdelaR) during 2000−2005 is also gratefully acknowledged. The authors thank the Laboratory of Evolution (FC-UdelaR) for lending the descriptive analysis software. E.L.C. is indebted to Dr. A. Romerosa (University of Almería, Spain) for firstly attracting her attention into the world of transition metal-based drugs.

Supporting Information Available: Detailed information on structure and anticancer activity indices (Tables S1 and S2), theoretical descriptors and predictors calculated for the complete set of compounds at the level of theory employed in this work (Table S3), and shape and energetics of LUMO and LUMO+1 KS orbitals for **6**, **7**, **13**, and **15** (Figure 1S). This material is available free of charge via the Internet at http://pubs.acs.org.

REFERENCES AND NOTES

(1) Wang, D.; Lippard, S. J. Cellular Processing of Platinum Anticancer Drugs. *Nature Rev. Drug Discovery* **2005**, *4*, 307–320. (b) Kelland, L. The resurgence of platinum-based cancer chemoteraphy. *Nature Rev. Cancer* **2007**, *7*, 573–584. (c) Arnesano, F.; Natile, G. Mechanistic insight into the cellular uptake and processing of cisplatin 30 years after its approval by FDA. *Coord. Chem. Rev.* **2009**, in press. doi: 10.1016/j.ccr.2009.01.028.

(2) Gregg, R. W.; Molepo, J. M.; Monpetit, V. J. A.; Mikael, N. Z.; Redmond, D.; Gadia, M. Cisplatin neurotoxicity: the relationship between dosage, time, and platinum concentration in neurologic tissues, and morphologic evidence of toxicity. *J. Clin. Oncol.* **1992**, *10*, 795–803.

(3) Bloemink, M. J.; Reedijk, J. Cisplatin and derived anticancer drugs: mechanism and current status of DNA binding. In *Metal ions in biological systems, vol. 32*; Sigel, A.; Sigel, H. Eds.; Dekker: New York 1996, 641−685.

(4) Fink, D.; Howell, S. B. How does Cisplatin kill cells? In *Platinum-Based Drugs in Cancer Therapy*; Kelland, L. R., Farrell, N. P., Eds.; Humana Press: NJ, 2000; pp 149−167. (b) Brabec, V.; Kasparkova, J. Molecular aspects of resistance to antitumor platinum drugs. *Drug Resistance Updates* **2002**, *5*, 147–161. (c) Kartalou, M.; Essigmann, J. Mechanisms of resistance to cisplatin. *Mutat. Res.* **2001**, *478*, 23–43. (d) Rabik, C. A.; Dollan, M. E. Molecular mechanisms of resistance and toxicity associated with platinating agents. *Cancer Treat. Rev.* **2007**, *33*, 9–23.

(5) Highley M. S.; Calvert, A. H. Clinical experience with Cisplatin and Carboplatin. In *Platinum-Based Drugs in Cancer Therapy*; Kelland, L. R., Farrell N. P., Eds.; Humana Press: NJ, 2000; pp 171−194.

(6) Carr, J. L.; Tingle, M. D.; McKeage, M. J. Satraplatin activation by haemoglobin, cytochrome C and liver microsomes in vitro. *Cancer Chemother. Pharmacol.* **2006**, *57*, 483–490. (b) Hall, M. D.; Dillon, C. T.; Zhang, M.; Beale, P.; Cai, Z.; Lai, B.; Stampfl, A. P. J.; Hambley, T. W. The cellular distribution and oxidation state of platinum(II) and platinum(IV) antitumour complexes in cancer cells. *J. Biol. Inorg. Chem.* **2003**, *8*, 726–732.

(7) Galanski, M.; Jakupec, M. A.; Keppler, B. K. Update of the Preclinical Situation of Anticancer Platinum Complexes: Novel Design Strategies and Innovative Analytical Approaches. *Curr. Med. Chem.* **2005**, *12*, 2075–2094. (b) Jakupec, M. A.; Galanski, M.; Keppler, B. K. Tumour-inhibiting platinum complexes-state of the art and future perspectives. *Rev. Physiol. Biochem. Pharmacol.* **2003**, *146*, 1–53. (c) Wong, E.; Giandomenico, C. M. Current Status of Platinum Based Antitumor Drugs. *Chem. Rev.* **1999**, *99*, 2451–2466.

(8) McKeage, M. J. Clinical toxicology of platinum-based cancer chemotherapeutic agents. In *Platinum-Based Drugs in Cancer Therapy*; Kelland, L. R., FarrellN. P., Eds.; Humana Press: NJ, 2000; pp 251−276. (b) Graham, J.; Mushin, M.; Kirkpatrick, P. Fresh from the Pipeline: Oxaliplatin. *Nat. Rev. Drug Discovery* **2004**, *3*, 11–12.

(9) Fojo, T.; Farrell, N.; Ortuzar, W.; Tanimura, H.; Weinstein, J.; Myers, T. G. Identification of non-cross-resistant platinum compounds with novel cytotoxicity profiles using the NCI anticancer drug screen and clustered image map visualization. *Crit. Rev. Oncol./Hematol.* **2005**, *53*, 25–34. (b) Ziegler, C. J.; Silverman, A. P.; Lippard, S. J. High-throughput synthesis and screening of platinum drug candidates. *J. Biol. Inorg. Chem.* **2000**, *5*, 774–783. (c) Sandman, K. E.; Lippard, S. J. Methods for screening the potential antitumor activity of platinum compounds in combinatorial libraries. In *Cisplatin: Chemistry and Biochemistry of a Leading Anticancer Drug*; Lippert, B., Ed.; Wiley-VCH: Zürich, 1999; pp 523−536. (d) Huang, R.; Wallqvist, A.; Covell, D. G. Anticancer metal compounds in NCI's tumor-screening database: putative mode of action. *Biochem. Pharmacol.* **2005**, *69*, 1009–1039.

(10) Lippert, B. Trans-diammineplatinum(II): What makes it different form cis-DDP? Coordination chemistry of a neglected relative of Cisplatin and its interaction with nucleic acids. In *Metal ions in biological systems, vol. 33*; Sigel, A., Sigel, H., Eds.; Dekker: New York, 1996; pp 105−141.

(11) Rosenberg, B. Platinum complexes for the treatment of cancer: Why the search goes on. In *Cisplatin: Chemistry and Biochemistry of a Leading Anticancer Drug*; Lippert, B., Ed.; Wiley-VCH: Zürich, 1999; pp 3−30. (b) Cleare, M. J.; Hoeschele, J. D. Antitumor Platiunum Compounds. Relation between Structure and Activity. *Plat. Met. Rev.* **1973**, *17*, 2–13. (c) Cleare, M. J.; Hoeschele, J. D. Studies on the Antitumor Activity of Group VIII Transition Metal Complexes. Part I. Platinum(II) Complexes. *Bioinorg. Chem.* **1973**, *2*, 187–210.

(12) Natile, G.; Coluccia, M. Current status of trans-platinum compounds in cancer therapy. *Coord. Chem. Rev.* **2001**, *216−217*, 383–410.

(13) Holford, J.; Raynaud, F.; Murrer, B. A.; Grimaldi, K.; Hartley, J. A.; Abrams, M.; Kelland, L. R. Chemical, biochemical and pharmacological activity of the novel sterically hindered platinum co-ordination complex, cis-[amminedichloro(2-methylpyridine-)]platinum(II) (AMD473). *Anti-Cancer Drug Des.* **1998**, *13*, 1–18. (b) Kelland, L. R.; Sharp, S. Y.; O'Neill, C. F.; Raynaud, F. I.; Beale, P. J.; Judson, I. R. Mini-review: discovery and development of platinum complexes designed to circumvent cisplatin resistance. *J. Inorg. Biochem.* **1999**, *77*, 111–115. (c) Holford, J.; Beale, P. J.; Boxall, F. E.; Sharp, S. Y.; Kelland, L. R. Mechanism of drug resistance to the platinum complex ZD0473 in ovarian cancer cell lines. *Eur. J. Cancer* **2000**, *36*, 1984–1990. (d) Kawamura-Akiyawa, Y.; Kusaba, H.; Kanzawa, F.; Tamura, T.; Saijo, N.; Nishio, K. Non-cross resistance of ZD0473 in acquired cisplatin-resistant lung cancer cell lines. *Lung Cancer* **2002**, *38*, 43–59. (e) Sharp, S. Y.; O'Neill, C. F.; Boxall, F. E.; Kelland, L. R. Retention of activity by the new generation platinum agent AMD0473 in four human tumour cell lines possessing acquired resistance to oxaliplatin. *Eur. J. Cancer* **2002**, *38*, 2309–2315.

(14) Kelland, L. R. New platinum drugs: The pathway to oral therapy. In *Platinum-Based Drugs in Cancer Therapy*; Kelland, L. R., FarrellN. P., Eds.; Humana Press: NJ, 2000; pp 299−320. (b) Choy, H.; Park, C.; Yao, M. Current Status and Future Prospects for Satraplatin and Oral Platinum Analogue. *Clin. Cancer Res.* **2008**, *14*, 1633–1638.

(15) Farrell, N. P. Polynuclear charged platinum compounds as a new class of anticancer agents: Toward a new paradigm. In *Platinum-Based Drugs in Cancer Therapy*; Kelland, L. R., Farrell N. P., Eds.; Humana Press: NJ, 2000; pp 321−338.

(16) Butour, J. L.; Wimmer, S.; Wimmer, F.; Castan, P. Palladium(II) compounds with potential antitumour properties and their platinum analogues: a comparative study of the reaction of some orotic acid derivatives with DNA in vitro. *Chem. Biol. Interact.* **1997**, *104*, 165–178. (b) Mansuri-Torshizi, H.; Ghadimy, S.; Akbarzadeh, N. Synthesis, characterization, DNA binding and cytotoxic studies of platinum(II) and palladium(II) complexes of the 2−2′-bipyridine and an anion of 1,1-cyclobutanedicarboxylic acid. *Chem. Pharm. Bull.* **2001**, *49*, 1517–1520. (c) Gao, E.; Sun, Y.; Liu, Q.; Duan, L. An anticancer metallobenzylmalonate: crystal structure and anticancer activity of a palladium complex of 2,2′-bipyridine and benzylmalonate. *J. Coord. Chem.* **2006**, *59*, 1295–1300. (d) Divsalar, A.; Saboury, A. A.; Yousefi, R.; Moosavi-Movahedi, A. A.; Mansoori-Torshizi, H. Spectroscopic and cytotoxic studies of the novel designed palladium(II) complexes: β-lactoglobulin and K562 as the targets. *Int. J. Biol. Macromol.* **2007**, *40*, 381–396. (e) Pucci, D.; Bellusci, A.; Bernardini, S.; Bloise, R.; Crispini, A.; Federici, G.; Liguori, P.; Lucas, M. F.; Russo, N.; Valentini, A. Bioactive fragments synergically involved in the design of new generation Pt(II) and Pd(II)-based anticancer compounds. *Dalton Trans.* **2008**, 5897–5904. (f) Garoufis, A.; Hadjikakou, S. K.; Hadjiliadis, N. Palladium coordination compounds as anti-viral, anti-fungal, anti-microbial and anti-tumor agents. *Coord. Chem. Rev.* **2009**, *253*, 1384–1397.

(17) Chval, Z.; Sip, M. Pentacoordinated transition states of cisplatin hydrolysis-ab initio study. *J. Mol. Struct. (Theochem)* **2000**, *532*, 59–68. Burda, J. V.; Zeizinger, M.; Šponer, J.; Leszczynski, J. Hydration of cis- and trans-platin: A pseudopotential treatment in the frame of a G3-type theory for platinum complexes. *J. Chem. Phys.*

2000, *113*, 2224–2232. Bergès, J.; Caillet, J.; Langlet, J.; Kozelka, J. Hydration and 'inverse hydration' of platinum(II) complexes: an analysis using the density functionals PW91 and BLYP. *Chem. Phys. Lett.* **2001**, *344*, 573–577. (d) Zhang, Y.; Guo, Z.; You, X. Hydrolysis theory for Cisplatin and its analogues based on Density Functional studies. *J. Am. Chem. Soc.* **2001**, *123*, 9378–9387. (e) Tsipis, A. C.; Sigalas, M. P. Mechanistic aspects of the complete set of hydrolysis and anation reactions of cis- and trans-DDP related to their antitumor activity modeled by an improved ASED-MO approach. *J. Mol. Struct. (Theochem)* **2002**, *584*, 235–248. (f) Costa, L. A. S.; Rocha, W. R.; De Almeida, W. B.; Dos Santos, H. F. The hydrolysis process of the cis-dichloro(ethylendiamine)platinum(II): A theoretical study. *J. Chem. Phys.* **2003**, *118*, 10584–10592. (g) Costa, L. A. S.; Rocha, W. R.; De Almeida, W. B.; Dos Santos, H. F. The solvent effect on the aquation processes of the cis-dichloro-(ethylenediammine)platinum(II) using continuum solvation models. *Chem. Phys. Lett.* **2004**, *387*, 182–187. (h) Burda, J. V.; Zeizinger, M.; Leszczynski, J. Activation barriers and rate constants for hydration of platinum and palladium square-planar complexes: An *ab initio* study. *J. Chem. Phys.* **2004**, *120*, 1253–1262. (i) Robertazzi, A.; Platts, J. A. Hydrogen bonding, solvation and hydrolysis of Cisplatin: A theoretical study. *J. Comput. Chem.* **2004**, *25*, 1060–1067. (j) Raber, J.; Zhu, C.; Eriksson, L. A. Activation of anti-cancer drug Cisplatin-is the activated complex fully aquated. *Mol. Phys.* **2004**, *102*, 2537–2544. (k) Zhu, C.; Raber, J.; Eriksson, L. A. Hydrolysis process of the second generation platinum-based anticancer drug cis-Amminedichlorocyclohexylamineplatinum(II). *J. Phys. Chem. B* **2005**, *109*, 12195–12205. (l) Lau, J. K.-C.; Deubel, D. V. Hydrolysis of the anticancer drug Cisplatin: Pitfalls in the interpretation of quantum chemical calculations. *J. Chem. Theory Comput.* **2006**, *2*, 103–106. (m) Song, T.; Hu, P. Insight into the solvent effect: A density functional theory study of Cisplatin hydrolysis. *J. Chem. Phys.* **2006**, *125*, 091101−1-3. (n) Pavelka, M.; Lucas, M.F. A.; Russo, N. On the hydrolysis mechanism of the second-generation anticancer drug Carboplatin. *Chem.—Eur. J.* **2007**, *13*, 10108–10116. (o) Yuan, Q.; Zhou, L.; Gao, Y. The hydrolysis mechanism of the anticancer agent trans-dichloro(ammine)(quinoline) platinum complex: a theoretical study. *J. Theoret. Comput. Chem.* **2008**, *7*, 381–395. (p) Lopes, J. F.; Rocha, W. R.; Dos Santos, H. F.; De Almeida, W. B. Theoretical study of the potential energy surface for the interaction of cisplatin and their aquated species with water. *J. Chem. Phys.* **2008**, *128*, 165103−1-14.

(18) Boudreaux, E. A.; Carsey, T. P. Quasirelativistic MO calculations on platinum complexes (anticancer drugs) and their interaction with DNA. *Int. J. Quantum Chem.* **1980**, *18*, 469–479. (b) Basch, H.; Krauss, M.; Stevens, W. J.; Cohen, D. Binding of $Pt(NH_3)_3^{2+}$ to nucleic acid bases. *Inorg. Chem.* **1986**, *25*, 684–688. (c) Zilberberg, I. L.; Avdeev, V. I.; Zhidomirov, G. M. Effect of cisplatin binding on guanine in nucleic acid: an ab initio study. *J. Mol. Struct. (Theochem)* **1997**, *418*, 73–81. (d) Pelmenschikov, A.; Zilberberg, I. L.; Leszczynski, J.; Famulari, A.; Sironi, M.; Raimondi, M. cis-[Pt(NH3)2]2+ coordination to the N7 and O6 sites of a guanine-cytosine pair: disruption of the Watson-Crick H-bonding pattern. *Chem. Phys. Lett.* **1999**, *314*, 496–500. (e) Burda, J. V.; Sponer, J.; Leszczynski, J. The interactions of square platinum(II) complexes with guanine and adenine: a quantum-chemical ab initio study of metalated tautomeric forms. *J. Biol. Inorg. Chem.* **2000**, *5*, 178–188. (f) Burda, J. V.; Šponer, J.; Leszczynski, J. The influence of square planar platinum complexes on DNA base pairing. An *ab initio* DFT study. *Phys. Chem. Chem. Phys.* **2001**, *3*, 4404–4411. (g) Baik, M.-H.; Friesner, R. A.; Lippard, S. Theoretical study on the stability of *N*-glycosyl bonds: Why does N7-platination not promote depurination. *J. Am. Chem. Soc.* **2002**, *124*, 4495–4503. (h) Baik, M.-H.; Friesner, R. A.; Lippard, S. J. Theoretical study of Cisplatin binding to purine bases: Why does Cisplatin prefer Guanine over Adenine. *J. Am. Chem. Soc.* **2003**, *125*, 14082–14092. (i) Burda, J. V.; Šponer, J.; Hrabáková, J.; Zeizinger, M.; Leszczynski, J. The influence of N_7 Guanine modifications on the strength of Watson-Crick base pairing and Guanine N_1 acidity: Comparison of Gas-Phase and Condensed-Phase Trends. *J. Phys. Chem. B* **2003**, *107*, 5349–5356. (j) Burda, J. V.; Leszczynski, J. How strong can the bend be on a DNA helix from Cisplatin? DFT and MP2 quantum chemical calculations of Cisplatin-bridged DNA purine bases. *Inorg. Chem.* **2003**, *42*, 7162–7172. (k) Zeizinger, M.; Burda, J. V.; Leszczynski, J. The influence of a sugar-phosphate backbone on the cisplatin-bridged BpB′ models of DNA purine bases. Quantum chemical calculations of Pt(II) bonding characteristics. *Phys. Chem. Chem. Phys.* **2004**, *6*, 3585–3590. (l) Gu, J.; Wang, J.; Leszczynski, J. H-bonding patterns in the platinated Guanine-Cytosine base pair and Guanine-Cytosine-Guanine-Cytosine base tetrad: an electron density deformation analysis and AIM study. *J. Am. Chem. Soc.* **2004**, *126*, 12651–12660. (m) Robertazzi, A.; Platts, J. A. Hydrogen bonding and covalent effects in binding of Cisplatin to purine bases: ab initio and Atoms in Molecules studies. *Inorg. Chem.* **2005**, *44*, 267–274. (n) Raber, J.; Zhu, C.; Eriksson, L. A. Theoretical study of Cisplatin binding to DNA: the importance of initial complex stabilization. *J. Phys. Chem. B* **2005**, *109*, 11006–11015. (o) Jia, M.; Qu, W.; Yang, Z.; Chen, G. Theoretical study on the factors that affect the structure and stability of the adduct of a new platinum anticancer drug with a duplex DNA. *Int. J. Modern Phys. B* **2005**, *19*, 2939–2949. (p) Costa, L. A.; Hambley, T. W.; Rocha, W. R.; Almeida, W. B.; Dos Santos, H. F. Kinetics and structural aspects of the cisplatin interactions with guanine: A quantum mechanical description. *Int. J. Quantum Chem.* **2006**, *106*, 2129–2144. (q) Robertazzi, A.; Platts, J. A. Gas-phase DNA Oligonucleotide structures. A QM/MM and Atoms in Molecules study. *J. Phys. Chem. A* **2006**, *110*, 3992–4000. (r) Robertazzi, A.; Platts, J. A. A QM/MM study of Cisplatin-DNA oligonucleotides: from simple models to realistic systems. (s) Matsui, T.; Shigeta, Y.; Hirao, K. Influence of Pt complex binding on the guanine-cytosine pair: a theoretical study. *Chem. Phys. Lett.* **2006**, *423*, 331–334. (t) Matsui, T.; Shigeta, Y.; Hirao, K. Multiple proton-transfer reactions in DNA base pairs by coordination of Pt complex. *J. Phys. Chem. B* **2007**, *111*, 1176–1181. (u) Mantri, Y.; Lippard, S. J.; Baik, M.-H. Bifunctional binding of cisplatin to DNA: Why does cisplatin form 1,2-intrastrand cross-links with AG but not with GA? *J. Am. Chem. Soc.* **2007**, *129*, 5023–5030. (v) Andrushchenko, V.; Wieser, H.; Bouř, P. DNA Oligonucleotide-cisplatin binding: ab initio interpretation of the vibrational spectra. *J. Phys. Chem. A.* **2007**, *111*, 9714–9723. (w) Pavelka, M.; Burda, J. V. Pt-bridges in various single-strand and double-helix DNA sequences. DFT and MP2 study of the cisplatin coordination with guanine, adenine, and cytosine. *J. Mol. Mod.* **2007**, *13*, 367–379. (x) Hao, L.; Li, X. C.; Tan, H. W.; Chen, G. J.; Jia, M. X. Energy basis of recognition of base pair for platinum-based antitumor drug ZD0473 and cisplatin. *Sci. China Ser. B-Chem.* **2008**, *51*, 4359–366.

(19) Deubel, D. V. On the competition of the purine bases, functionalities of peptide side chains, and protecting agents for the coordination sites of dicationic Cisplatin derivatives. *J. Am. Chem. Soc.* **2002**, *124*, 5834–5842. (b) Deubel, D. V. Factors governing the kinetic competition of nitrogen and sulfur ligands in Cisplatin binding to biological targets. *J. Am. Chem. Soc.* **2004**, *126*, 5999–6004. (c) Lau, K. C.; Deubel, D. V. Loss of ammine from platinum(II) complexes: Implications for Cisplatin inactivation, storage, and resistance. *Chem.—Eur. J.* **2005**, *11*, 2849–2855. (d) Zimmermann, T.; Zeizinger, M.; Burda, J. V. Cisplatin interaction with cysteine and methionine, a theoretical DFT study. *J. Inorg. Biochem.* **2005**, *99*, 2184–2196. (e) Summa, N.; Schiessi, W.; Puchta, R.; van Eikema Hommes, N.; van Eldik, R. Thermodynamic and kinetic studies on reactions of Pt(II) complexes with biologically relevant nucleophiles. *Inorg. Chem.* **2006**, *45*, 2948–2959. (f) Alberto, M. E.; Lucas, M. F.; Pavelka, M.; Russo, N. The degradation pathways in chloride medium of the third generation anticancer drug Oxaliplatin. *J. Phys. Chem.* **2008**, *112*, 10765–10768. (g) Chojnacki, H.; Kuduk-Jaworska, J.; Jaroszewicz, I.; Jański, J. J. In silico approach to cisplatin toxicity. Quantum chemical studies on platinum(II)-cysteine systems. *J. Mol. Model.* **2009**, in press, doi 10.1007/s00894−009−0469−2.

(20) Carloni, P.; Sprik, M.; Andreoni, W. Key steps of the *cis*-platin-DNA interaction: Density Functional Theory-based Molecular Dynamics simulations. *J. Phys. Chem. B* **2000**, *104*, 823–835. (b) Spiegel, K.; Rothlisberger, U.; Carloni, P. Cisplatin binding to DNA oligomers from hybrid Car-Parrinello/Molecular Dynamics simulations. *J. Phys. Chem. B* **2004**, *108*, 2699–2707. (c) Magistrato, A.; Ruggerone, P.; Spiegel, K.; Carloni, P.; Reedjik, J. Binding of novel azole-bridged dinuclear Platinum(II) anticancer drugs to DNA: Insights from hybrid QM/MM Molecular Dynamics simulations. *J. Phys. Chem. B* **2006**, *110*, 3604–3613. (d) Spiegel, K.; Magistrato, A.; Carloni, P.; Reedijk, J.; Klein, M. L. Azole-bridged diplatinum anticancer compounds. Modulating DNA flexibility to escape repair mechanism and avoid cross resistance. *J. Phys. Chem.* **2007**, *111*, 11873–11876.

(21) Kozelka, J. Computational studies on Platinum antitumor complexes and their adducts with nucleic-acid constituents. In *Cisplatin. Chemistry and Biochemistry of a Leading Anticancer Drug*; Lippert, B., Ed.; Wiley-VCH: Weinheim, Germany, 1999; pp 537−556. (b) Scheeff, E. D.; Briggs, J. M.; Howell, S. B. Molecular modelling of the intrastrand Guanine-Guanine DNA adducts produced by Cisplatin and Oxaliplatin. *Mol. Pharmacol.* **1999**, *56*, 633–643. (c) Hambley, T. W.; Jones, A. W. Molecular mechanics modeling of Pt/nucleotide and Pt/DNA interactions. *Coord. Chem. Rev.* **2001**, *212*, 35–59. (d) Elizondo-Riojas, M. A.; Kozelka, J. Unrestrained 5 ns Molecular Dynamics simulation of a Cisplatin-DNA 1,2-GG adduct provides a rationale for the NMR features and reveals increased conformational flexibility at the platinum binding site. *J. Mol. Biol.* **2001**, *314*, 1227–1243. (e) Kasparkova, J.; Delalande, O.; Stros, M.; Elizondo-Riojas, M.-A.; Vojtiskova, M.; Kozelka, J.; Brabec, V. Recognition of DNA interstrand cross-link of antitumor cisplatin by HMGB1 protein. *Biochemistry* **2003**, *42*, 1234–1244. (f) Delalande, O.; Malina, J.; Brabec, V.;

Kozelka, J. Chiral Differentiation of DNA adducts formed by enantiomeric analogues of antitumor Cisplatin is sequence-dependent. *J. Biophys. J.* **2005**, *88*, 4159–4169. (g) Sharma, S.; Gong, P.; Temple, B.; Bhattacharyya, D.; Dokholoyan, N. V.; Chaney, S. G. Molecular Dynamic simulations of Cisplatin- and Oxaliplatin-d(GG) intrastrand cross-links reveal differences in their conformational dynamics. *J. Mol. Biol.* **2007**, *373*, 1123–1140.

(22) Abdul-Ahad, P. G.; Webb, G. A. Quantitative Structure Activity Relationships for some antitumor Platinum(II) complexes. *Int. J. Quantum Chem.* **1982**, *21*, 1105–1115. (b) Platts, J. A.; Hibbs, D. E.; Hambley, T. W.; Hall, M. D. Calculation of the Hydrophobicity of Platinum Drugs. *J. Med. Chem.* **2001**, *44*, 472–474. (c) Tsipis, A. C.; Katsoulos, G. A. Conformational preferences, rotational barriers and energetics of purine nucleobase rotation and dissociation in square planar platinum(II) antitumour complexes: Structure-activity correlation. *Phys. Chem. Chem. Phys.* **2001**, *3*, 5165–5172. (d) Saunders, R. A.; Platts, J. A. Scaled Polar Surface Area Descriptors: Development and application to three sets of Partition Coefficients. *New J. Chem.* **2004**, *28*, 166–172. (e) Costa, L. A.; Rocha, W. R.; Almeida, W. B.; Dos Santos, H. F. Linear free energy relationship for 4-substituted (o-phenylenediamine)platinum(II) dichloride derivatives using quantum mechanical descriptors. *J. Inorg. Biochem.* **2005**, *99*, 575–583. (f) Oldfield, S. P.; Hall, M. D.; Platts, J. A. Calculation of lipophilicity of a large, diverse dataset of anticancer platinum complexes and the relation to cellular uptake. *J. Med. Chem.* **2007**, *50*, 5227–5237. (g) Bradac, O.; Zimmerman, T.; Burda, J. V. Comparison of the electronic properties, and thermodynamic and kinetic parameters of the aquation of selected platinum(II) derivatives with their anticancer IC_{50} indexes. *J. Mol. Model.* **2008**, *14*, 705–716. (h) Sarmah, P.; Deka, R. C. Solvent effect on the reactivity of cis-platinum(II) complexes: A density functional approach. *Int. J. Quantum Chem.* **2008**, *108*, 1400–1409.

(23) Yoshida, M.; Khokhar, A. R.; Siddik, Z. H. Cytotoxicity and tolerance to DNA adducts of alicyclic mixed amines platinum(II) homologs in tumor models sensitive and resistant to cisplatin or tetraplatin. *Oncol. Rep.* **1998**, *5*, 1281–1287. (b) Siddik, Z. H.; Thai, G.; Yoshida, M.; Zhang, Y. P.; Khokhar, A. R. Tetravalent platinum complexes with ammine/amine carrier ligand configuration: circumvention of platinum resistance in vivo. *Anti-Cancer Drug Des.* **1994**, *9*, 495–509.

(24) Vollano, J. F.; Al-Baker, S.; Dabrowiak, J. C.; Schurig, J. E. Comparative Antitumor Studies on Platinum(II) and Platinum(IV) Complexes Containing 1,2-Diaminocyclohexane. *J. Med. Chem.* **1987**, *30*, 716–719.

(25) Monti, E.; Gariboldi, M.; Maiocchi, A.; Marengo, E.; Cassino, C.; Gabano, E.; Osella, D. Cytotoxicity of cis-platinum(II) conjugate models. The effect of chelating arms and leaving groups on cytotoxicity: a quantitative structure-activity relationship approach. *J. Med. Chem.* **2005**, *48*, 857–866.

(26) Luo, F. R.; Wyrick, S. D.; Chaney, S. G. Comparative neurotocixity of oxaliplatin, ormaplatin, and their biotransformation products utilizing a rat dorsal root ganglia in vitro explant culture model. *Cancer Chemother. Pharmacol.* **1999**, *44*, 29–38.

(27) Screnci, D.; McKeage, M. J.; Galettis, P.; Hambley, T. W.; Palmer, B. D.; Baguley, B. C. Relationships between hydrophobicity, reactivity, accumulation and peripheral nerve toxicity of a series of platinum drugs. *Br. J. Cancer* **2000**, *82*, 966–972.

(28) Clark, D. L.; Andrews, P. A.; Smith, D. D.; De George, J. J.; Justice, R. L.; Beitz, J. G. Predictive value of preclinical toxicology studies for platinum anticancer drugs. *Clin. Cancer Res.* **1999**, *5*, 1161–1167.

(29) Fokkema, E.; Groen, H. J. M.; Helder, M. N.; de Vries, E. G. E.; Meijer, C. JM216-, JM118-, and cisplatin-induced cytotoxicity in relation to platinum-DNA adduct formation, glutathione levels and p53 status in human tumour cell lines with different sensitivities to cisplatin. *Biochem. Pharmacol.* **2002**, *63*, 1989–1996. (b) Samini, G.; Kishimoto, S.; Manorek, G.; Breaux, J. K.; Howell, S. B. Novel mechanisms of platinum drug resistance identified in cells selected for resistance to JM118 the active metabolite of satraplatin. *Cancer Chemother. Pharmacol.* **2007**, *59*, 301–312.

(30) Hoeschele, J. D.; Showalter, H. D.; Kraker, A. J.; Elliott, W. L.; Roberts, B. J.; Kampf, J. W. Synthesis, structural characterization, and antitumor properties of a novel class of large-ring platinum(II) chelate complexes incorporating the cis-1,4-diaminocyclohexane ligand in a unique locked boat conformation. *J. Med. Chem.* **1994**, *37*, 2630–2636. (b) Shamsuddin, S.; Takahashi, I.; Siddik, Z. H.; Khokhar, A. R. Synthesis, Characterization, and Antitumor Activity of a Series of Novel Cisplatin Analogs with the cis-1,4-Diaminocyclohexane as Nonleaving Amine Group. *J. Inorg. Biochem.* **1996**, *61*, 291–301.

(31) Monk, B. J.; Alberts, D. S.; Burger, R. A.; Fanta, P. T.; Hallum III, A. V.; Hatch, K. D.; Salmon, S. E. In vitro phase II comparison of the cytotoxicity of a novel platinum analog, nedaplatin (254-S), with that of cisplatin and carboplatin against fresh, human cervical cancers. *Gynecol. Oncol.* **1998**, *71*, 308–312. (b) Kanzawa, F.; Koizumi, F.; Koh, Y.; Nakamura, T.; Tatsumi, Y.; Fukumoto, H.; Saijo, N.; Yoshioka, T.; Nishi, K. In vitro synergistic interactions between the cisplatin analogue nedaplatin and the DNA topoisomerase I inhibitor irinotecan and the mechanism of this interaction. *Clin. Cancer Res.* **2001**, *7*, 202–209.

(32) Becke, A. D. Density-functional thermochemistry. III. The role of exact exchange. *Chem. Phys.* **1993**, *98*, 5648–5652. (b) Lee, C.; Yang, W.; Parr, R. G. Development of the Colle-Salvetti correlation-energy formula into a functional of the electron density. *Phys. Rev. B* **1988**, *37*, 785–789.

(33) Ditchfield, R.; Hehre, W. J.; Pople, J. A. Self-Consistent Molecular-Orbital Methods. IX. An Extended Gaussian-Type Basis for Molecular-Orbital Studies of Organic Molecules. *J. Chem. Phys.* **1971**, *54*, 724–728.

(34) DunningT. H., Jr.; Hay, P. J. Gaussian basis sets for molecular calculations. In *Modern Theoretical Chemistry*; Schaefer, H. F., III, Ed.; Plenum, NY, 1976; Vol. 3, pp 1−28. (b) Hay, P. J.; Wadt, W. R. Ab initio effective core potentials for molecular calculations. Potentials for the transition metal atoms Sc to Hg. *J. Chem. Phys.* **1985**, *82*, 270–283. (c) Hay, P. J.; Wadt, W. R. Ab initio effective core potentials for molecular calculations. Potentials for K to Au including the outermost core orbitals. *J. Chem. Phys.* **1985**, *82*, 299–310.

(35) Cancès, M. T.; Mennucci, B.; Tomasi, J. A new integral equation formalism for the polarizable continuum model: Theoretical background and applications to isotropic and anisotropic dielectrics. *J. Chem. Phys.* **1997**, *107*, 3032–3041. (b) Tomasi, J.; Mennucci, B.; Cancès, E. The IEF version of the PCM solvation method: an overview of a new method addressed to study molecular solutes at the QM ab initio level. *J. Mol. Struct. (Theochem)* **1999**, *464*, 211–226.

(36) Barone, V.; Cossi, M.; Mennuci, B.; Tomasi, J. A new definition of cavities for the computation of solvation free energies by the polarizable continuum model. *J. Chem. Phys.* **1997**, *107*, 3210–3221.

(37) (a) Pavankumar, P. N. V.; Seetharamulu, P.; Yao, S.; Saxe, J. D.; Reddy, D. G.; Hausheer, F. H. Comprehensive ab initio quantum mechanical and molecular orbital (MO) analysis of cisplatin: Structure, bonding, charge density, and vibrational frequencies. *J. Comput. Chem.* **1999**, *20*, 365–382. (b) Wysokinski, R.; Michalska, D. The performance of different Density Functional methods in the calculation of molecular structures and vibrational spectra of Platinum(II) antitumor drugs: Cisplatin and Carboplatin. *J. Comput. Chem.* **2001**, *22*, 901–912. (c) Dans, P.; Crespo, A.; Estrín, D. A.; Coitiño, E. L. Structural and energetic study of Cisplatin and derivatives: comparison of the performance of DFT implementations. *J. Chem. Theory Comput.* **2008**, *4*, 740–750.

(38) Reed, A. E.; Curtiss, L. A.; Weinhold, F. Intermolecular interactions from a natural bond orbital, donor-acceptor viewpoint. *Chem. Rev.* **1988**, *88*, 899–926.

(39) Geerlings, P.; De Prof, F.; Langenaeker, W. Conceptual Density Functional Theory. *Chem. Rev.* **2003**, *103*, 1793–1874.

(40) Frisch, M. J.; Trucks, G. W.; Schlegel, H. B.; Scuseria, G. E.; Robb, M. A.; Cheeseman, J. R.; Zakrzewski, V. G.; Montgomery, J. A.; Stratmann, R. E.; Burant, J. C.; Dapprich, S.; Millam, J. M.; Daniels, A. D.; Kudin, K. N.; Strain, M. C.; Farkas, O.; Tomasi, J.; Barone, V.; Cossi, M.; Cammi, R.; Mennucci, B.; Pomelli, C.; Adamo, C.; Clifford, S.; Ochterski, J.; Petersson, G. A.; Ayala, P. Y.; Cui, Q.; Morokuma, K.; Malick, D. K.; Rabuck, A. D.; Raghavachari, K.; Foresman, J. B.; Cioslowski, J.; Ortiz, J. V.; Baboul, A. G.; Stefanov, B. B.; Liu, G.; Liashenko, A.; Piskorz, P.; Komaromi, I.; Gomperts, R.; Martin, R. L.; Fox, D. J.; Keith, T.; Al-Laham, M. A.; Peng, Y.; Nanayakkara, A.; Challacombe, M.; Gill, P. M. W.; Johnson, B.; Chen, W.; Wong, M. W.; Andres, J. L.; Gonzalez, C.; Head-Gordon, M.; Replogle, E. S.; Pople, J. A. Gaussian Inc.: Pittsburgh, PA, 1998. (b) *GaussView rev. 2.1*; Gaussian Inc.: Pittsburgh, PA, 2000.

(41) Portmann, S. *Molekel 4.3 for Linux*; CSCS/ETHZ: Geneva, Copyright 2000−2002. (b) Fluekiger, P. F. *Molekel IRIX-GL original implementation, concept and data structure*; CSCS/UNI: Geneva, 2000.

(42) Ward, J. H. Hierarchical grouping to optimize an objective function. *J. Am. Statist. Asoc.* **1963**, *58*, 236–244. (b) Downs, G. M.; Barnard, J. M. Clustering Methods and Their Uses in Computational Chemistry. In *Reviews in Computational Chemistry*; Lipkowitz, K. B., Boyd, D. B., Eds.; Wiley-VCH, John Wiley & Sons: 2002; Vol. 18, pp 1−40. (c) Martin, Y. C.; Bures, M. G.; Brown, R. D. Validated descriptors for diversity measurements and optimization. *Pharm. Pharmacol. Comm.* **1998**, *4*, 147–152.

(43) *Electronic Statistics Textbook*; StatSoft Inc., Tulsa, OK. http://www.statsoft.com/textbook/stathome.html (accessed Feb 18, 2009). (b) James, F. C.; McCulloch, C. E. Multivariate analysis in ecology and systematics: Panacea or Pandora's Box? *Annu. Rev. Ecol. Syst.* **1990**, *21*, 129–166.

(44) Boon, G.; Langenaeker, W.; De Prof, F.; De Winter, H.; Tollenaere, J. P.; Geerlings, P. Systematic Study of the Quality of Various Quantum Similarity Descriptors. Use of the Autocorrelation Function and Principal Component Analysis. *J. Phys. Chem. A* **2001**, *105*, 8805–8814.

(45) *STATISTICA (data analysis software system), release 6.0*; StatSoft, Inc., Tulsa, OK, Copyright 1984−2008. http://www.statsoft.com/ (accessed Feb 18, 2009).

(46) Hofmann, A.; Jaganyi, D.; Munro, O. Q.; Liehr, G.; van Eldik, R. Electronic Tuning of the Lability of Pt(II) Complexes through π-Acceptor Effects. Correlations between Thermodynamic, Kinetic, and Theoretical Parameters. *Inorg. Chem.* **2003**, *42*, 1688–1700. (b) Baik, M.-H.; Friesner, R. A.; Lippard, S. J. Cis-$[Pt(NH_3)_2(L)]^{2+/+}$ (L = Cl, H_2O, NH_3) Binding to Purines and CO: Does π-Back-Donation Play a Role? *Inorg. Chem.* **2003**, *42*, 8615–8617. (c) Romeo, R.; Plutino, M. R.; Scolaro, L. M.; Stoccoro, S.; Minghetti, G. Role of Cyclometalation in Controlling the Rates of Ligand Substituttion at Platinum(II) Complexes. *Inorg. Chem.* **2000**, *39*, 4749–4755. (d) Reddy, D.; Jaganyi, D. Does increased chelation enhance the rate of ligand substitution at Pt^{II}(N, N, N) centres? A detailed kinetic & mechanistic study. *Transition Metal Chem.* **2006**, *31*, 792–800.

(47) (a) Stordal, B.; Pavlakis, N.; Davey, R. Oxaliplatin for the treatment of cisplatin-resistant cancer: A systematic review. *Cancer Treat. Rev.* **2007**, *33*, 347–357. (b) Desoize, B.; Madoulet, C. Particular aspects of platinum compounds used at present in cancer treatment. *Crit. Rev. Oncol./Hemat.* **2002**, *42*, 317–325.

(48) Reedjik, J. New clues for platinum antitumor chemistry: Kinetically controlled metal binding to DNA. *Proc. Natl. Acad. Sci.* **2003**, *100*, 3611–3616. (b) Fuertes, M. A.; Alonso, C.; Pérez, J. M. Biochemical modulation of Cisplatin mechanisms of action: enhancement of antitumor activity and circumvention of drug resistance. *Chem. Rev.* **2003**, *3*, 645–662. (c) Pereira-Maia, E.; Garnier-Soullerot, A. Impaired hydrolysis of cisplatin derivatives to aquated species prevents energy-dependent uptake in GLC4 cells resistant to cisplatin. *J. Biol. Inorg. Chem.* **2003**, *8*, 626–634. (d) Martelli, L.; Di Mario, F.; Ragazzi, E.; Apostoli, P.; Leone, R.; Perego, P.; Fumagalli, G. Different accumulation of cisplatin, oxaliplatin and JM216 in sensitive and cisplatin-resistant human cervical tumour cells. *Biochem. Pharmacol.* **2006**, *72*, 693–700.

(49) Safaei, R.; Howell, S. B. Copper Transporters regulate the cellular pharmacology and sensitivity to Pt drugs. *Crit. Rev. Oncol/Hematol.* **2005**, *53*, 13–23. (b) Holzer, A. K.; Manorek, G. H.; Howell, S. B. Contribution of the Major Copper Influx Transporter CTR1 to the Cellular Accumulation of Cisplatin, Carboplatin, and Oxaliplatin. *Mol. Pharmacol.* **2006**, *70*, 1390–1394. (c) Samimi, G.; Howell, S. B. Modulation of the cellular pharmacology of JM118, the major metabolite of satraplatin, by copper influx and efflux transporters. *Cancer Chemother. Pharm.* **2006**, *57*, 781–788. (d) Zisowsky, J.; Koegel, S.; Leyers, S.; Devarakonda, K.; Kassack, M. U.; Osmack, M.; Jaehde, U. Relevance of drug uptake and efflux for cisplatin sensitivity of tumor cells. *Biochem. Pharmacol.* **2007**, *73*, 298–307.

(50) Zhang, S.; Lovejoy, K. S.; Shima, J. E.; Lagpacan, L. L.; Shu, Y.; Lapuk, A.; Chen, Y.; Komori, T.; Gray, J. W.; Chen, X.; Lippard, S. J.; Giacomini, K. M. Organic Cation Transporters are Determinants of Oxaliplatin Cytotoxicity. *Cancer Res.* **2006**, *66*, 8847–8857. (b) Yonezawa, A.; Masuda, S.; Yokoo, S.; Katsura, T.; Inui, K. Cisplatin and Oxaliplatin, but Not Carboplatin and Nedaplatin, Are Substrates for Human Organic Cation Transporters (SLC22A1−3 and Multidrug and Toxin Extrusion Family). *J. Pharmacol. Exp. Ther.* **2006**, *319*, 879–886. (c) Yokoo, S.; Yonezawa, A.; Masuda, S.; Fukatsu, A.; Katsura, T.; Inui, K. Differential contribution of organic cation transporters, OCT2 and MATE1, in platinum agent-induced nephrotoxicity. *Biochem. Pharmacol.* **2007**, *74*, 477–487.

CI800421W